Simulation of Reverse Short Channel Effects with a Consistent Point-Defect Diffusion Model

Hironori Sakamoto, Shigetaka Kumashiro, *Masayuki Hiroi,
*Masami Hane, and *Hiroshi Matsumoto
ULSI Device Development Laboratories, NEC Corporation,
*Microelectronics Research Laboratories, NEC Corporation
1120 Shimokuzawa, Sagamihara, Kanagawa 229, Japan
Tel:+81-427-79-9927 Fax:+81-427-71-0938 E-mail:h-saka@lsi.tmg.nec.co.jp

Abstract – A consistent point-defect diffusion model including the impurity clustering was implemented, and the reverse short channel effect(RSCE) strength of the nMOSFETs was compared with the pMOSFETs using a common model parameter set. As the result of simulations for typical single-drain MOSFETs, the RSCE was calculated in the nMOSFETs but not in the pMOSFETs. The reason of this RSCE difference is that in the nMOSFETs the interstitials are generated during the arsenic(As) clustering process in the source/drain(S/D) region, but in the pMOSFETs the interstitials are absorbed during the boron(B) clustering process. It is clarified that this interstitial generation or absorption plays a significant role in the difference of the RSCE between nMOSFETs and pMOSFETs.

I. INTRODUCTION

It has been widely accepted that channel boron(B) re-distribution which is caused by the point-defect generation due to the S/D implantation is responsible for the RSCE. It is not well-understood why the strong RSCE is observed in nMOSFETs but not in pMOSFETs. Although many RSCE simulations using a point-defect diffusion model have been reported so far, most of them used specially fitted parameter sets to reproduce RSCE [1] and there has been no consistent explanation of the origin of the RSCE difference between nMOSFETs and pMOSFETs. In this paper, a consistent point-defect diffusion model for B, phosphorus(P) and As was implemented and the RSCE strength of the nMOSFETs was compared with the pMOSFETs using a common model parameter set.

II. MODEL AND PARAMETERS

A set of point-defect diffusion model including clustering effect [2-4] was applied to B, P and As. B cluster($B_{cl} = \sum_n n B_{cl}^{(n)}$) was assumed to be an accumulation of boron-interstitial(BI) pairs and As_2V and As_3 components [4] were assumed for As clusters. Both {311} cluster($I_{cl} = \sum_n n I_{cl}^{(n)}$) [5] and sink term due to ion implantation damage were taken into account. The reactions considered in this model are:

$$B + I \rightleftharpoons BI \quad (1)$$
$$BI + V \rightleftharpoons B \quad (2)$$
$$BI + BI \rightleftharpoons B_{cl}^{(2)} \quad (3)$$
$$B_{cl}^{(n)} + BI \rightleftharpoons B_{cl}^{(n+1)} \quad (4)$$
$$P + I \rightleftharpoons PI \quad (5)$$
$$P + V \rightleftharpoons PV \quad (6)$$
$$PI + V \rightleftharpoons P \quad (7)$$
$$PV + I \rightleftharpoons P \quad (8)$$
$$As + I \rightleftharpoons AsI \quad (9)$$
$$As + V \rightleftharpoons AsV \quad (10)$$
$$AsI + V \rightleftharpoons As \quad (11)$$
$$AsV + I \rightleftharpoons As \quad (12)$$
$$As + AsV \rightleftharpoons As_2V \quad (13)$$
$$As_2V + AsI \rightleftharpoons As_3 \quad (14)$$
$$I + V \rightleftharpoons \phi \quad (15)$$
$$I + I \rightleftharpoons I_{cl}^{(2)} \quad (16)$$
$$I_{cl}^{(n)} + I \rightleftharpoons I_{cl}^{(n+1)} \quad (17)$$

The initial excess point-defect concentration was assumed to be zero in the amorphous region and "+1" in the other region as shown in Fig.1. Here, the amorphous

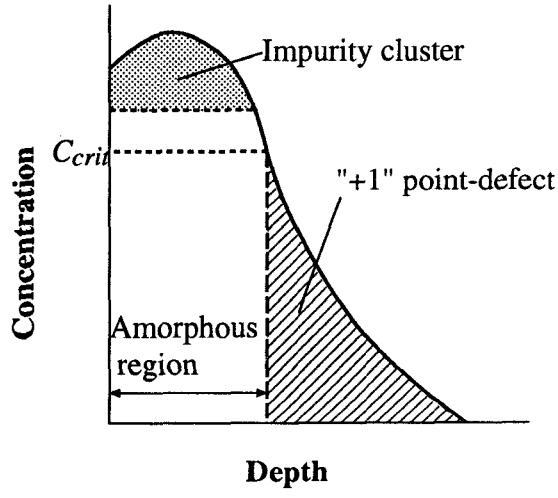

Fig.1: Initial condition after the implantation.

0-7803-3775-1/97/$10.00 © 1997 IEEE.

region was defined as the region where the implanted impurity concentration was larger than the critical concentration C_{crit}. The value of C_{crit} depends on the implanted ion and $3 \times 10^{19}\text{cm}^{-3}$ for As^+ and $2 \times 10^{20}\text{cm}^{-3}$ for BF_2^+ were used according to the TEM measurements. In the amorphous region the part of impurities whose concentration exceeded $3 \times 10^{20}\text{cm}^{-3}$ for As and $2 \times 10^{20}\text{cm}^{-3}$ for B were assumed to be the cluster. The initial As cluster was assumed to be As_3.

The model parameters were determined so that the simulation results should agree with experimental 1D profiles. For example, the simulated and the measured profiles of the n-type and the p-type MOSFET S/D regions are shown in Figs.2 and 3, respectively. The simulated B

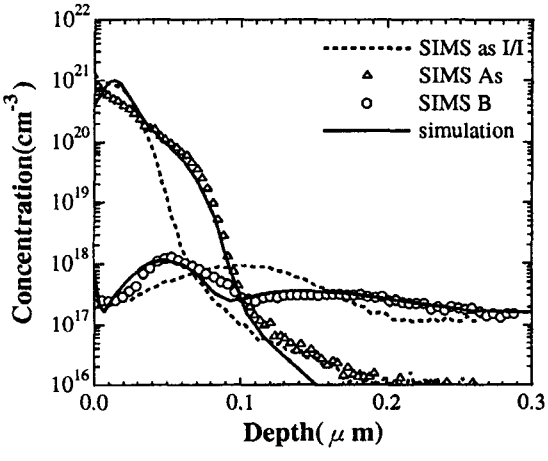

Fig.2: Simulated and measured profiles after B 30keV $1 \times 10^{13}\text{cm}^{-2}$ + As 30keV $3 \times 10^{15}\text{cm}^{-2}$ implantation followed by 850°C 60 min anneal.

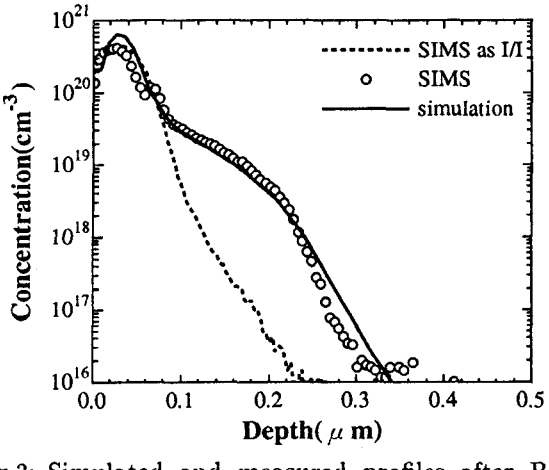

Fig.3: Simulated and measured profiles after BF_2 50keV $3 \times 10^{15}\text{cm}^{-2}$ implantation followed by 850°C 60 min anneal.

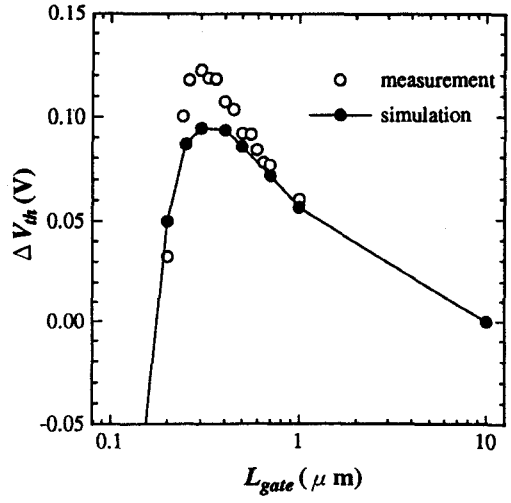

Fig.4: Simulated and measured ΔV_{th}-L_{gate} characteristics of the nMOSFETs.

profiles in these figures agree well with the measurement. Therefore, it is clear that the relative strength of the transient enhanced diffusion near the n-type and the p-type S/D regions can be well reproduced by the extracted model parameters. It was also confirmed that the RSCE simulation result of actual nMOSFETs by using these parameters agreed with the measurement within 30mV error as shown in Fig.4.

III. SIMULATION

In order to compare the RSCE of the nMOSFETs with the pMOSFETs, simulations were performed for typical single-drain MOS device structures using the common model parameter set described above. In the case of the nMOSFETs, the following two conditions were also compared using the same initial point-defect distribution.

(a) The point-defect diffusion model was used for all impurities (B, P and As).

(b) The conventional Fermi-level dependent diffusion model was used for As instead of the point-defect diffusion model (reactions (9)-(14)).

The same thermal budget was used for both the nMOSFETs and the pMOSFETs. The ion implantation conditions and the LDD sidewall thickness were determined so that the profiles and the effective channel lengths of the nMOSFETs coincided with those of the pMOSFETs. The concrete values are shown table 1.

Table 1: Device structures and process conditions of typical nMOSFETs and pMOSFETs.

	nMOSFETs	pMOSFETs
Channel I/I	B 30keV $1 \times 10^{13}cm^{-2}$	P 100keV $1 \times 10^{13}cm^{-2}$
Anneal	1000°C 10 sec	
Sidewall thickness	8nm	13nm
S/D I/I	As 40keV $3 \times 10^{15}cm^{-2}$	BF_2 30keV $3 \times 10^{15}cm^{-2}$
S/D anneal	800°C 60 min	

IV. RESULTS AND DISCUSSION

Simulation results of V_{th}-L_{gate} characteristics are shown in Fig.5. The nMOSFETs show the RSCE, while there is no RSCE in the pMOSFETs. In the case of the nMOSFETs(b), the RSCE is very weak. By examining the changes of the impurity (B for the nMOSFETs and P for the pMOSFETs) profiles at the mid-channel according to the L_{gate} (Figs.7-9), it is clear that the difference in the RSCE strength is calculated due to the difference in the impurity re-distribution.

For quantitative discussion, the enhancement factors of the diffusion constants $\langle D_{eff} \rangle / D_{intr}$ in the channel are calculated and shown in Fig.10. Here, $\langle D_{eff} \rangle$ and D_{intr} represent the time averaged effective diffusion constant and the intrinsic diffusion constant, respectively. In the case of the nMOSFETs(a), the enhancement factor of the diffusion constant is four times larger than in the case of the pMOSFETs, while they are similar between the nMOSFETs(b) and the pMOSFETs. Since both B and P diffuse mainly via interstitial mechanism [2,3], the following relation is obtained:

$$\langle D_{eff} \rangle / D_{intr} \simeq \int C_I / C_I^* dt.$$

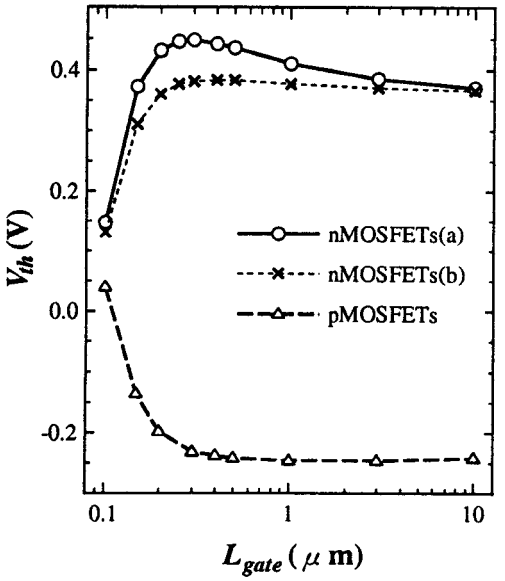

Fig.5: Simulated V_{th}-L_{gate} characteristics of typical nMOSFETs and pMOSFETs.

Therefore, the large enhancement factor of the diffusion constant in the nMOSFETs(a) is attributed to its higher excess interstitial amount. However, the initial interstitial amount in the pMOSFETs is seven times larger than the one in the nMOSFETs, because the ranges of the amorphous region are different.

These phenomena can be consistently explained as follows. The difference between nMOSFETs(a) and nMOSFETs(b) is due to the interstitial generation described by the reaction (12) which is subsequently caused by AsV and As_2V cluster formation in the highly doped As region. In other word, the As in the S/D region emits interstitials when some part of it becomes inactive. Recently, this phenomenon has been confirmed experimentally as well by P. M. Rousseau *et al.* [6]. The significantly smaller enhancement factor of the pMOSFETs compared with the nMOSFETs(a) is due to the interstitial absorption described by the reaction (1),(3) and (4) which correspond to the B cluster formation in the highly doped B region. In contrast to As, the B in the S/D region absorbs interstitials during its deactivation process. This difference in the interstitial related clustering plays a significant role in the RSCE simulation.

V. CONCLUSION

A consistent point-defect diffusion model using a common model parameter set is developed for both nMOSFETs and pMOSFETs. It is clarified that there are two origins of the RSCE difference between nMOSFETs and pMOSFETs. One is the interstitial generation caused by the As clustering process in the nMOSFETs. Another one is the interstitial absorption caused by the B clustering process in the pMOSFETs.

ACKNOWLEDGMENT

The authors would like to thank Dr. S. Asada for his continual support and encouragement. The authors would also like to thank K. Shimizu, M. Ohsugi, and Y. Kawashima for the SIMS measurements, and N. Sugawara and S. Ohyama for the measurements of the electric characteristics.

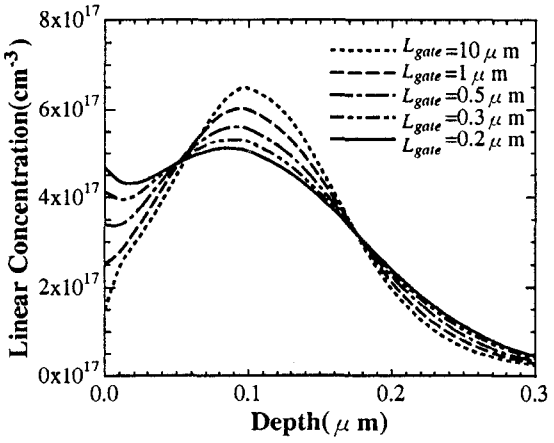

Fig.7: Change of the B profiles at the mid-channel of the nMOSFETs(a) according to the L_{gate}.

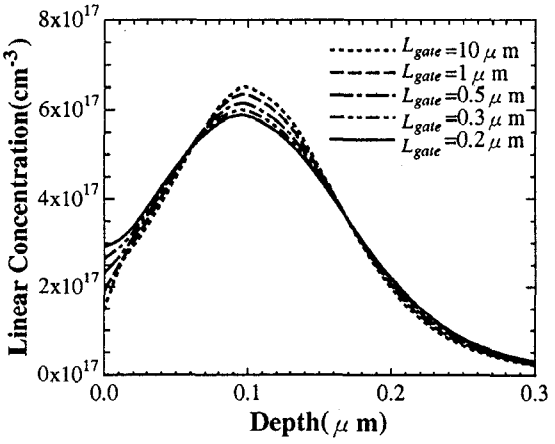

Fig.8: Change of the B profiles at the mid-channel of the nMOSFETs(b) according to the L_{gate}.

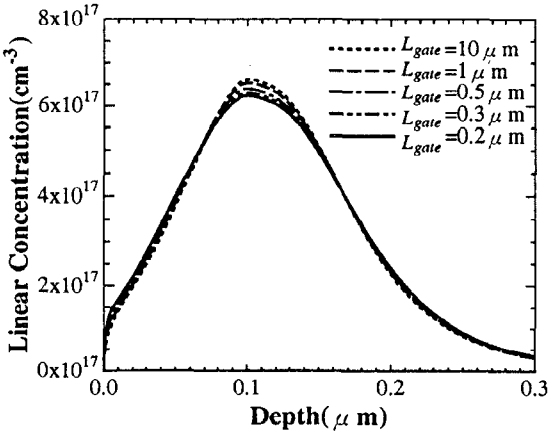

Fig.9: Change of the P profiles at the mid-channel of the pMOSFETs according to the L_{gate}.

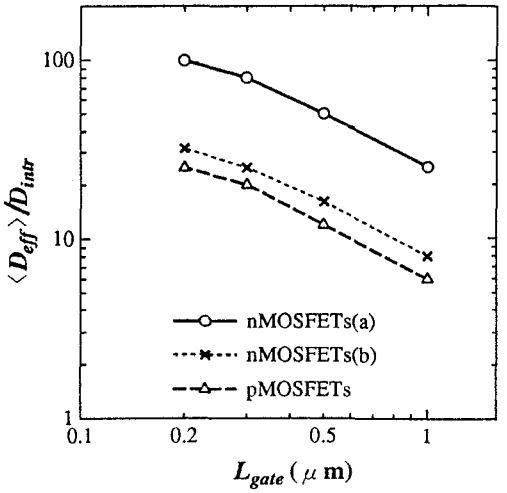

Fig.10: Variation of $\langle D_{eff} \rangle / D_{intr}$ according to the L_{gate}.

REFERENCES

[1] F. Lau, P. Küpper, and K. H. Gebhardt, "Two-Dimensional Calibration of Dopant Transport Models for Submicron CMOS transistors", SISPAD'96, Tokyo, Japan, pp.111-112, 1996.

[2] M. Hane, T. Ikezawa, M. Hiroi, and H. Matsumoto, "Dopant Diffusion Model Refinement and its Impact on the Calculation of Reverse Short Channel Effect", IEDM Tech. Digs., pp.803-806, 1996.

[3] Sc. T. Dunham, "A Quantitative Model for the Coupled Diffusion of Phosphorus and Point Defects in Silicon", J. Electrochem. Soc., vol.139, No.9, pp.2628-2636, 1992.

[4] M. Hiroi, T. Ikezawa, M. Hane, and H. Matsumoto, "A Pair-Diffusion Model for Arsenic in Silicon Considering Arsenic Deactivation-Induced Interstitial-Silicon Emission", MRS, 1997 spring, *to be published.*

[5] C. S. Rafferty, G. H. Gilmer, M. Jaraiz, D. Eaglesham, and H. -J. Gossmann, "Simulation of Cluster Evaporation and Transient enhanced Diffusion in Silicon", Appl. Phys. Lett., vol.68, No.17, pp.2395-2397, 1996.

[6] P. M. Rousseau, S. W. Crowder, P. B. Griffin, and J. D. Plummer, "Arsenic Deactivation Enhanced Diffusion and the Reverse Short-Channel Effect," IEEE Electron Device Letters, vol.18, No.2, pp.42-44, 1997.